JOM, Vol. 71, No. 3, 2019
https://doi.org/10.1007/s11837-019-03339-5
© 2019 The Minerals, Metals & Materials Society

Effects of Varying Heat Treatments on the Microstructure and Mechanical Properties of Blown Powder Inconel 625

MYLES D. FULLEN[1,2] and JUDY A. SCHNEIDER[1]

1.—Department of Mechanical and Aerospace Engineering, University of Alabama in Huntsville, Huntsville, AL 35899, USA. 2.—e-mail: mylesfullen4@gmail.com

Blown powder deposition (BPD) is an additive manufacturing (AM) technique which builds components in a layer by layer fashion. In BPD AM, metal powder is fed through nozzles into the path of a laser beam which is attached to a robotic arm. This increases the size of the build envelope beyond the limitations of powder-bed AM systems. After fabrication, the specimens are subjected to various heat treatments to relieve residual stresses and optimize the mechanical properties. As AM processing is relatively new, heat treatment standards are still being developed. Key to standardization is obtaining an understanding of the key parameters by evaluating differences in BPD materials built by different vendors. This study evaluates the effects of varying heat treatments on the mechanical response of Inconel 625 specimens obtained from four different vendors.

INTRODUCTION

Inconel 625 is a nickel (Ni)-based superalloy, used for applications in which corrosion resistance or retention of high strength at elevated temperatures is needed. These favorable properties have resulted in widespread usage in various industries such as aerospace, power, and medical. However, the same properties that are beneficial for high-temperature applications are not beneficial to many conventional forming and machining operations. Thus, with the emergence of additive manufacturing (AM) techniques for metals, Inconel 625 is a prime candidate. Inconel 625 alloy is fusion-weldable and available in many different forms including cast, powder metallurgy (PM), and wrought. Powders that have been developed for PM are readily available for use in various AM processes, including blown powder deposition (BPD). While much research has focused on optimization of the deposition parameters to achieve fully densified specimens, subsequent heat treatments must also be developed to optimize the properties.

Inconel 625 is a solid-solution-strengthened, Ni-based γ superalloy which contains carbides MC, M_6C or $M_{23}C_6$ that form either along grain boundaries or within grains.[1,2] The expected phases in the Inconel 625 system are summarized in Table I for the carbides in addition to possible nitride formations.[3–5] Development of heat treatments for AM Inconel 625 has relied on existing standards developed for wrought alloys[6] in which high strength is promoted in a fine-grained microstructure. Due to the rapid and repeated heating and cooling that occurs during AM processing, the resulting microstructure differs from that produced in casting or wrought materials. While there are standard heat treatments for traditional manufacturing methods, none exist for BPD AM of Inconel 625. Due to inherent residual stresses, AM materials are generally subjected to a stress-relief (SR) anneal cycle between 870°C and 900°C for 1 h. Following SR, it is recommended that wrought Inconel 625 be solution-annealed at a minimum temperature of 1093°C.[6,7] The solutionizing temperature can be increased to reduce the processing time, but is kept below 1160°C to avoid liquation of the eutectic MC phase.[2,7]

Several studies have evaluated the microstructural evolution after heat treatment of Inconel 625 specimens fabricated using powder-bed fusion (PBF) AM. In studies by Amato,[8] the only heat treatment was in hot isostatic pressing (HIP) at 1120°C, where full recrystallization of the microstructure was reported. In later studies by Li,[9] a range of temperatures were evaluated, with full recrystallization occurring at the solutioning temperature of 1150°C, similar to that reported by

(Published online January 18, 2019)

Marchese.[10] While PBF and BPD both utilize powder, the size of the feedstock typically varies from an average of 45 μm to 100 μm, respectively.[11,12] Due to the coarser powder size in BPD, the resulting microstructural response to heat treatment could vary from that observed in PBF. Very limited microstructure studies have been reported for BPD of Inconel 625. Dinda[12] conducted heat treatments at 1000°C, 1100°C, and 1200°C, with full recrystallization of a coarser microstructure only occurring at the highest temperature. In the reported heat treatment studies,[8–10,12] specimens were produced using one lot of powder on one AM machine. Thus, with the limited studies, it is not clear how variabilities may affect the observed results.

For this study, four vendors provided single-pass builds of Inconel 625 fabricated using BPD AM. A series of heat treatments were applied, and a comparison was made of the resulting microstructure and mechanical properties. By comparing the results of the heat treatments across specimens from different vendors, similarities and variabilities can be evaluated.

EXPERIMENTAL PROCEDURES

Single-pass, 3-mm-thick plates of Inconel 625 were manufactured by four different vendors using BPD AM. The plates were nominally 250 mm × 110 mm. Each plate was SR at 900°C for 1 h. The SR material was analyzed for elemental content using combustion analysis in accordance with ASTM E1019[13] to determine the carbon (C), sulfur (S), oxygen (O), and nitrogen (N) content. Inductively coupled plasma (ICP) analysis was used to determine all other elements in accordance with ASTM E1479.[14]

After the SR cycle, tensile specimens were removed from the plates with the remaining material cut into heat treat specimens of approximately 1 cm × 1 cm. The heat treat specimens were wrapped in stainless-steel foil and homogenized at three different temperatures for 3 h as summarized in Table II and air-cooled. Metallurgical specimens were mounted in two orientations, parallel to the build direction (Z) and perpendicular to the build direction (X–Y). The samples were mounted and metallographically prepared using standard practices with a final polish using 0.05-μm Al_2O_3. All specimens were imaged using a Zeiss XioVert.A1 m inverted microscope for reflected light techniques. Bright-field images were taken of the unetched specimens to record the void area, distribution, and morphology. ImageJ software was used for analysis of the images obtained. Sufficient images were recorded at 20 × magnification to obtain 100 voids, with indications less than six pixels or 2.7 μm rejected as noise. Based on the magnification, the numbers of pixels contained within the voids were used to directly determine the void area. The void areas were summed and divided by the number of pixels in the image to determine the percentage void area. After the void analysis, the specimens were etched by submersion in aqua regia to reveal the grain structure.

Electron discharge machining (EDM) was used to remove the tensile specimens from the build plate. The flat specimens had a cross-sectional width of 0.64 cm along a 3.2-cm gage length. A 0.95 cm radius transitioned the gage length to the 2.3-cm-wide grip region. All tensile tests were conducted on an Instron 5985 load frame. Calculation of stress was based on the loads obtained from a 250-kN load cell and specimen dimension measurements. All tests were run under displacement control at constant crosshead velocity of 0.13 cm/min per ASTM standard E8.[15] Three specimens were tested per orientation, per vendor in the SR condition only.

Hardness testing was conducted on each heat treatment specimen using a Wilson hardness tester on the Rockwell B scale. Average values were recorded from five or six indentations per specimen

Table I. Chemical formula and elemental composition of the phases within Inconel 625

Phase	Formula
γ	Ni
Nitrides[3–5]	(Nb,Ti,Cr)N
MC[1,2]	(Nb,Ti,Cr,Fe,Mo)C
M_6C[1,2]	$(Nb,Cr,Fe,Mo,Si)_6C$
$M_{23}C_6$[1,2]	$(Fe,Mo,Cr)_{23}C_6$
γ''[1,2]	$(Nb)Ni_3$

Table II. Heat treatment schedule

	Stress Relief (SR) (1 h)	Homogenization (3 h)		
	Specimen 1	Specimen 2	Specimen 3	Specimen 4
Vendor 1	900°C	SR + 1100°C	SR + 1125°C	SR + 1150°C
Vendor 2	900°C	SR + 1100°C	SR + 1125°C	SR + 1150°C
Vendor 3	900°C	SR + 1100°C	SR + 1125°C	SR + 1150°C
Vendor 4	900°C	SR + 1100°C	SR + 1125°C	SR + 1150°C

Table III. Elemental composition (wt.%)

	UNS N06625[6]	Vendor 1	Vendor 2	Vendor 3	Vendor 4
ICP analysis					
Ni	58.0 min	bal.	bal.	bal.	bal.
Cr	20.0–23.0	21.68	22.75	22.57	22.18
Mo	8.0–10.0	9.06	9.06	9.07	9.32
Nb	3.15–4.15	3.71	3.75	3.49	3.64
Ti	0.40 max	< 0.01	0.12	< 0.01	< 0.01
Al	0.40 max	0.04	0.13	0.03	0.03
Fe	5.0 max	1.17	0.77	**3.08**	0.75
Co	1.0 max	0.02	0.02	0.02	0.10
P	0.015 max	0.006	0.010	0.006	0.009
Mn	0.50 max	0.04	0.02	<0.01	0.21
Si	0.50 max	0.10	0.07	0.05	0.29
Combustion analysis					
C	0.10 max	0.01	0.03	0.02	0.01
S	0.015 max	0.003	0.002	0.001	0.003
N	–	**0.141**	0.0100	0.0109	**0.191**
O	–	0.0400	0.0561	0.0656	0.0546

per orientation. The hardness values were used to compare the effects of the heat treatment on the resulting mechanical properties.

RESULTS AND DISCUSSION

Table III summarizes the results of elemental analysis of the BPD specimens provided by the four vendors. While all specimens were within the UNS N06625[6] standard specifications, there were differences in the elemental composition of each, as highlighted in bold. The specimen from vendor 3 contained a significantly greater weight percentage of iron (Fe), while those from vendors 1 and 4 contained higher amounts of nitrogen (N): 0.141 wt.% and 0.1905 wt.%, respectively. In the absence of standard guidelines for the level of N content for Inconel 625, the content has been found to be < 0.005 wt.% in a survey of various Ni-based superalloys.[5]

A summary of the void area and percentage void area results is presented in Fig. 1a, b, c, and d, respectively. Void analysis of the unetched specimens considered both the relative area size and percentage void area for all the heat-treated specimens in the two orientations. The void analysis considered the pixels contained within the void to determine the area and then used that relative to the area of the image to obtain the percentage. Similar results were observed parallel to the build direction (Z) and perpendicular to the build plane (X–Y), indicating relatively circular voids. The specimens from vendors 2 and 4 had overall void areas of approximately 5 μm^2 with percentage void area of 0.50% to 0.75%. The void area and percentage void area remained fairly constant for the specimens from these two vendors across the heat treatment schedules evaluated. The specimen from vendor 1 showed a slight increase in void area from 5 μm^2 to 10 μm^2 with a corresponding increase in the percentage void area from 0.75% to 1.5% as the heat treatment temperature was increased. The largest void area increase of 10 μm^2 to 36.2 μm^2 was observed for the specimen from vendor 3 as the heat treatment temperature was increased. The corresponding increase in area correlated with a corresponding decrease in the percentage of void area. This increase in void area with a decrease in the percentage void area suggests that the voids in this sample experienced coalescence and growth as the temperature was increased.

After etching, optical images of the resulting microstructure were recorded for each heat treatment. Notable observations from the optical microscopy are summarized in Table IV. The specimens from each vendor responded differently to the same heat treatment parameters. The variation between the specimens from each vendor is most evident after the 1150°C heat treatment, as summarized in the corresponding micrographs in Fig. 2. Micrographs of the intermediate heat treatment temperatures are shown in the Electronic Supplementary material. Micrographs of the specimen from vendor 1 are shown in Supplementary Fig. S-1, those from vendor 2 in Supplementary Fig. S-2, those from vendor 3 in Supplementary Fig. S-3, and those from vendor 4 in Supplementary Fig. S-4.

Although the composition of Inconel 625 is fairly broad with no limits on the amount of O or N, evidence in literature suggests that the N content affects the microstructural response. Singh et al.[5] studied the effect of N on Inconel 625, finding that its presence increased formation of (Nb,Ti)N nitrides. The increased presence of (Nb,Ti)N was found to free C, promoting increased formation of $M_{23}C_6$ carbides along grain boundaries. $M_{23}C_6$

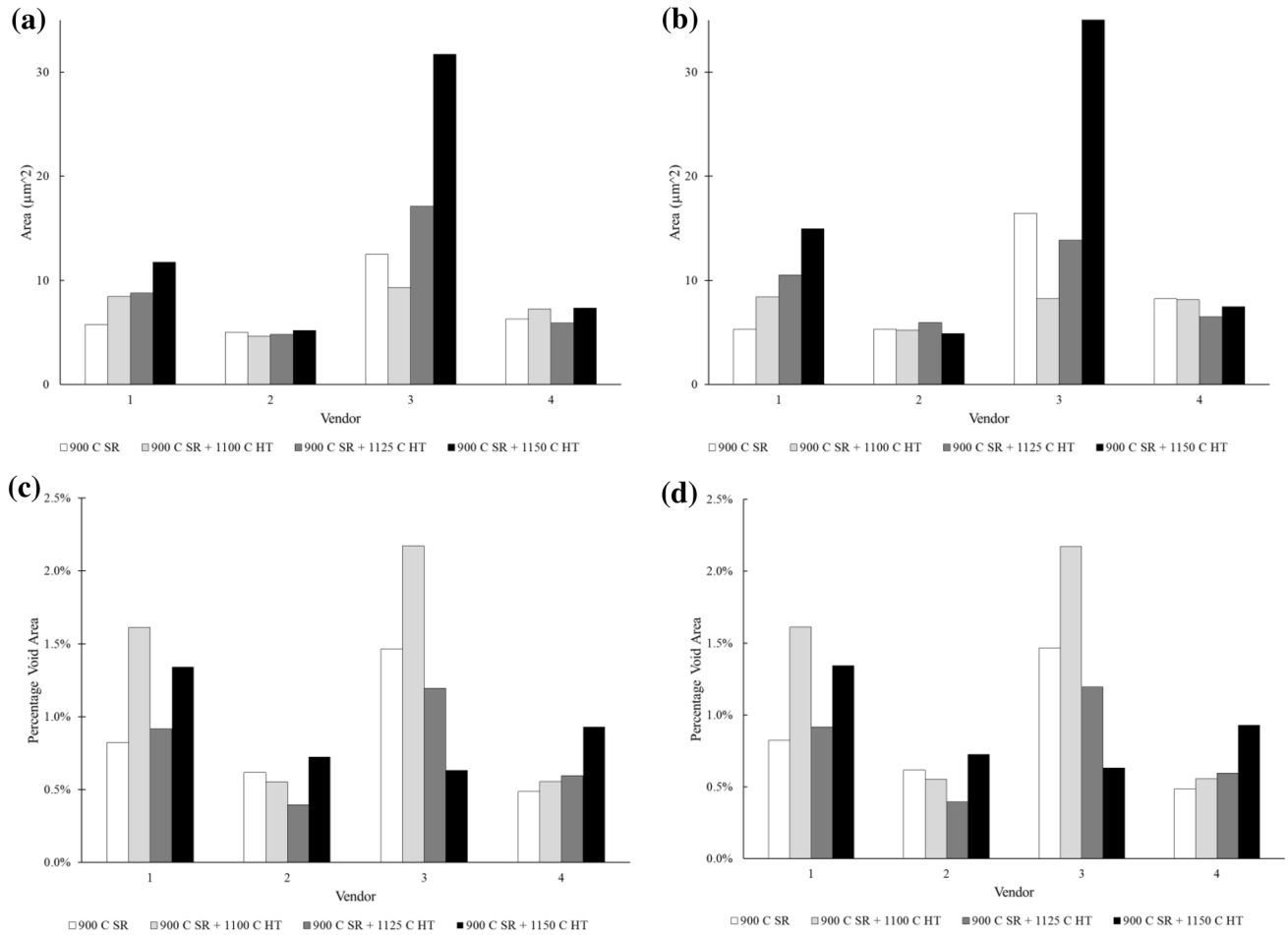

Fig. 1. Effect of heat treatment temperature on void area oriented (a) parallel to the build direction (*Z*) and (b) perpendicular to the build direction (*X*–*Y*), and as a percentage oriented (c) parallel to the build direction (*Z*) and (d) perpendicular to the build direction (*X*–*Y*).

Table IV. Microstructural observations per vendor

Vendor 1	Most significant recrystallization observed after 1100°C heat treatment followed by grain growth at higher heat treatment temperatures
Vendor 2	Similar degrees of recrystallization observed after 1100°C heat treatment, remaining consistent at higher heat treatment temperatures
Vendor 3	Initiation of recrystallization observed at the SR heat treatment, with increasing levels of recrystallization at higher heat treatment temperatures. Annealing twins appear after 1125°C, and their presence increases after 1150°C heat treatment
Vendor 4	No substantial recrystallization at any of the heat treatment temperatures

phase is known to be effective at pinning grain boundaries at lower temperatures. At temperatures above 1000°C, $M_{23}C_6$ phase dissolves back into the γ matrix.[5] The specimen from vendor 1 showed the second highest N content of 1.41 wt.%, which seems to correlate with the initial recrystallization followed by grain growth. The specimen from vendor 4 had the highest N content of 0.191 wt.% and displayed no evidence of recrystallization at any of the heat treatment temperatures investigated. Thus, it appears that the presence of N greatly affects the degree of recrystallization and the temperature at which it occurs.

The recrystallization observed in the specimen from vendor 2 remained relatively unchanged over the range of heat treatment temperatures investigated. Initial grain definition was observed after the 1100°C heat treatment, with more homogenization occurring after the 1150°C heat treatment without observed grain growth. The specimen from vendor

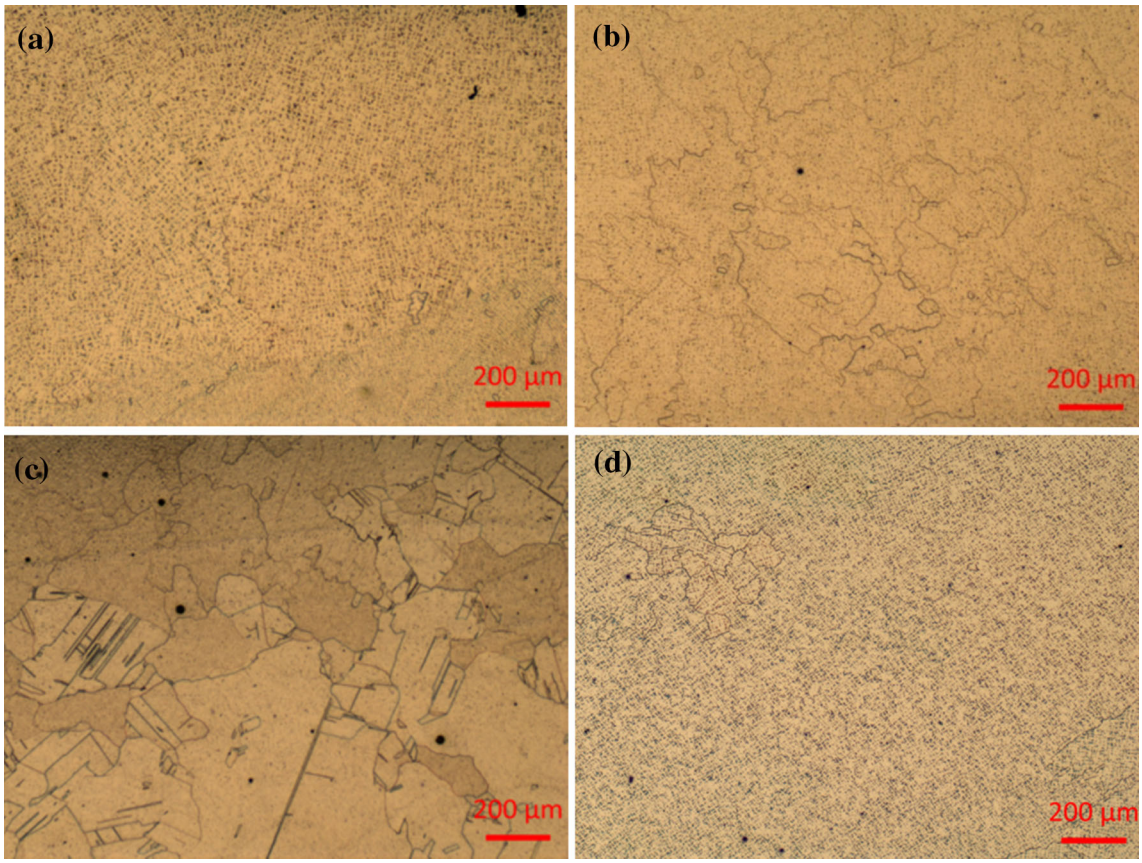

Fig. 2. Comparison of microstructure after stress relief and 1150°C homogenization heat treatment for specimens from vendor 1 (a), vendor 2 (b), vendor 3 (c), and vendor 4 (d).

3, which had the highest Fe content, showed increased degree of recrystallization as the heat treatment temperature was increased, which also promoted twinning. Twinning is an indication of recrystallization after residual stresses are partially relieved during heat treatment.[9] A recent study observing the microstructural evolution of Inconel 625 manufactured using PBF AM after various heat treatments found increased presence of twinning after 1150°C homogenization heat treatment. The metal powders used in Li's study[9] contained 4.1% Fe, which is approximately 1% higher than the specimen from vendor 3 and significantly higher than the specimens from the other vendors in this study. This study, along with the microstructural observations on the specimen from vendor 3, reveal a correspondence between the Fe content and twinning.

Tensile data from the samples undergoing only SR heat treatment are shown in Fig. 3a and b. As the specimens from all vendors exhibited differences in microstructural refinement after the heat treatment study, no further tension testing was performed at this time. The highest SR strength was observed for the specimens from vendors 1 and 4, which also had the highest N content. Higher content of N within the elemental composition of Inconel 625 has been shown to slightly increase the strength while decreasing the ductility.[4] It is possible that the increased N content resulted in more initial $M_{23}C_6$ formation at grain boundaries. As $M_{23}C_6$ dissolved at increasing temperatures, formation of M_6C carbides within the grains would be promoted, contributing to increased strengthening.

Despite the differences in void area between the specimens from vendors 2 and 3, they both had lower strength but increased ductility, especially when tested in the build direction. The specimens from vendors 1, 2, and 4 showed little change in hardness over the range of heat treatment temperatures investigated.

Softening at the 1150°C heat treatment temperature was most pronounced in the specimen from vendor 3, which had the highest degree of recrystallization. Such softening is expected when microstructures undergo recrystallization.[9,16,17] The weight percentage of Fe has also been shown to affect the microstructure and mechanical properties of Inconel 625. A study investigating the effects of Fe on AM Inconel 625 found that a higher percentage can cause a decrease in tensile strength with an increase in ductility.[18] This is primarily due

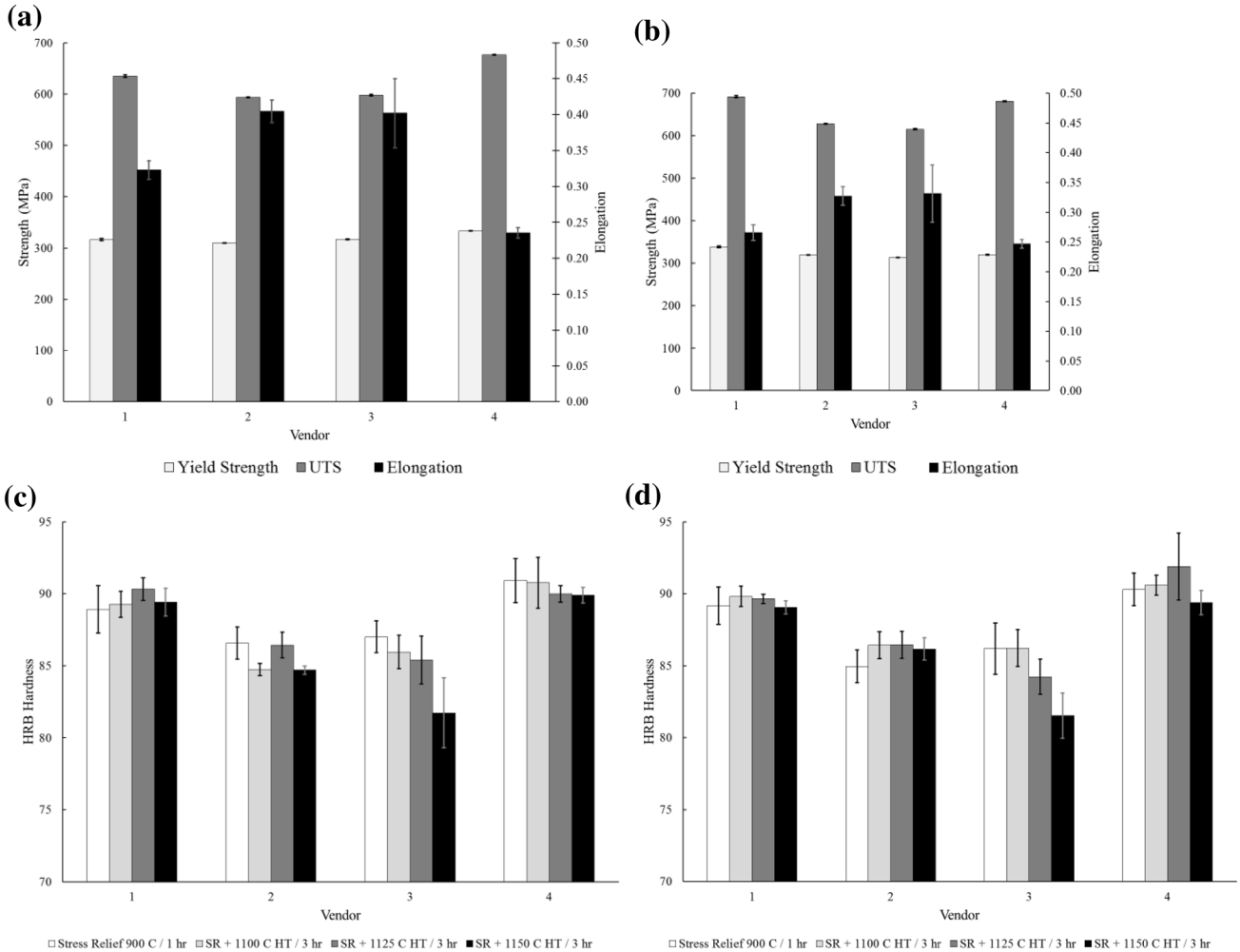

Fig. 3. Summary of mechanical properties of SR specimens oriented (a) parallel to the build direction (*Z*) and (b) perpendicular to the build direction (*X*–*Y*). Summary of hardness values following heat treatment at different temperatures in specimens oriented (c) parallel to the build direction (*Z*) and (d) perpendicular to the build direction (*X*–*Y*).

to the coarsening effect that Fe has on grains. While limited grain growth was observed in the specimens from vendor 3, the grains were coarser as compared with the specimens from vendors 1 and 2.

The vendors surveyed all used a laser to melt the deposited powder, although the initial source of the powder as well as the process parameters were unknown in this study. The high N levels in the specimens from vendors 1 and 4 may result from two possible sources. One would be residual N from the gas atomization process used to produce the powder. Argon (Ar) atomization is typically used with Ni-based superalloys, as N atomization is reported to form nitrides.[3–5] In the case of Inconel 625, N atomization could lead to formation of (Nb,Ti)N nitrides. Thus, a crucial step will be to obtain information regarding each vendor's powder supplier. Another potential source of N infiltration is the carrier gas during the BPD process. The metal powder is contained within a carrier gas before being blown into the laser beam. Commonly used carrier gases include Ar, He, and N. Use of N carrier gas could also lead to formation of (Nb,Ti)N nitrides. Future studies are recommended to acquire Inconel 625 powders from each vendor along with the AM-fabricated component for elemental analysis.

CONCLUSION

Inconel 625 manufactured using BPD can be used to fabricate larger-scale parts for applications in which high strength, corrosion resistance, or thermal resistance is needed. To recommend or standardize heat treatment parameters for this method, this study was conducted to analyze the response of BPD Inconel 625 to various heat treatments. Four vendors provided single-pass plates of Inconel 625, which revealed variability in microstructure and mechanical response after heat treatment at each temperature investigated.

The specimens from vendors 1 and 4 exhibited higher tensile strength and hardness, but lower ductility in SR condition. At higher temperatures, samples from both vendors experienced grain growth. This is linked to the higher percentage of N within the elemental composition, which frees C to form $M_{23}C_6$ carbides along grain boundaries at lower temperatures. At temperatures above 1000°C, $M_{23}C_6$ dissolves into the matrix, allowing grain growth.[13] These dissolved carbides in turn promote formation of M_6C carbides within the grain, which can increase the strength.

Increased ductility with lower tensile strength and hardness was observed in the specimens from vendors 2 and 3, which had lower levels of N, as compared with the specimens from vendors 1 and 4 in SR condition. Recrystallization was observed at higher temperatures, especially in the specimen from vendor 3, along with increased presence of Fe and annealing twins at higher temperatures.[9] The higher weight percentage of Fe in the specimen from vendor 3 also correlated to its slightly lower strength, increase in ductility, and coarse grain structure.[18]

The weight percentage of N affected the microstructural response of BPD Inconel 625 at the homogenization temperatures evaluated. This microstructural response also affects the mechanical properties of the material. Depending on recrystallization and the expected formation of C or N particles, there is a trade-off between grain pinning and creep versus fatigue life.[1,2,5] Based on the evidence from this study, it is recommended that post-build heat treatment parameters for BPD Inconel 625 be developed based upon the elemental composition of the material as well as the application.

ACKNOWLEDGEMENTS

The authors acknowledge funding provide by the Jacobs ESSSA Subcontract, NASA Grant NNM17AA02A. Specimens evaluated were provided by: DM3D, Formalloy, Joining Technologies, Alabama Laser, & RPMI.

CONFLICT OF INTEREST

The authors declare that they have no conflicts of interest.

ELECTRONIC SUPPLEMENTARY MATERIAL

The online version of this article (https://doi.org/10.1007/s11837-019-03339-5) contains supplementary material, which is available to authorized users.

REFERENCES

1. M. Sundararaman, P. Mukhopadhyay, and S. Banerjee, *Superalloys 718, 625, 706, and Various Derivatives*, 367 (1997).
2. S. Floreen, G.E. Fuchs, and W.J. Yang, *Superalloys 718, 625, 706, and Various Derivatives*, 13 (1994).
3. F.J. Rizzo, *JOM* 48, 24 (1996).
4. F.J. Rizzo, J.J. Conway, J.F. Radavich, and J.A. Jones, *Superalloys 718, 625, 706, and Various Derivatives*, 923 (1994).
5. J.B. Singh, A. Verma, B. Paul, and J.K. Chakravartty, *Eng. Failure Anal.* 32, 236 (2013).
6. ASTM B443, *Standard Specification for Nickel-Chromium-Molybdenum-Columbium Alloy (UNS N06625) and Nickel-Chromium-Molybdenum-Silicon Alloy (UNS N06219) Plate, Sheet, and Strip* (ASTM International, West Conshohocken, PA, 2014).
7. H.L. Eiselstein and D.J. Tillack, *Superalloys 718, 625, 706, and Various Derivatives*, 1 (1991).
8. K.N. Amato, J. Hernandez, L.E. Murr, E. Martinez, S.M. Gaytan, and P.W. Shindo, *J. Mater. Sci. Res.* 1, 3 (2012).
9. C. Li, R. White, X.Y. Fang, M. Weaver, and Y.B. Guo, *Mater. Sci. Eng. A* 705, 20 (2017).
10. G. Marchese, M. Lorusso, S. Parizia, E. Bassini, J. Lee, F. Calignano, D. Manfredi, M. Terner, H. Hong, D. Ugues, M. Lombardi, and S. Biamino, *Mater. Sci. Eng. A* 729, 64 (2018).
11. A.T. Sutton, C.S. Kriewall, M.C. Leu, and J.W. Newkirk, *Proceedings of the 27th Solid Freeform Fabrication Symposium*, 1004 (2016).
12. G.P. Dinda, A.K. Dasgupta, and J. Mazumder, *Mater. Sci. Eng. A* 509, 98 (2009).
13. ASTM E1019, *Standard Test Methods for Determination of Carbon, Sulfur, Nitrogen, and Oxygen in Steel, Iron, Nickel, and Cobalt Alloys by Various Combustion and Inert Gas Fusion Techniques* (ASTM International, West Conshohocken, PA, 2018).
14. ASTM E1479, *Standard Practice for Describing and Specifying Inductively Coupled Plasma Atomic Emission Spectrometers* (ASTM International, West Conshohocken, PA, 2016).
15. ASTM E8/E8M, *Standard Test Methods for Tension Testing of Metallic Materials* (ASTM International, West Conshohocken, PA, 2016).
16. D. Zhao, P.K. Chaudhury, R.B. Frank, and L.A. Jackman, *Superalloys 718, 625, 706, and Various Derivatives*, 315 (1994).
17. W.H. Cubberly, *Metals Handbook*, 9th ed. (Novelty, OH: ASM International, 1981), p. 655.
18. Z.R. Khayat and T.A. Palmer, *Mater. Sci. Eng. A* 718, 123 (2018).